International Journal of Engineering Technology Science and Research
IJETSR
www.ijetsr.com
ISSN 2394 – 3386
Volume 4, Issue 11
November 2017

Modeling and Simulation Infrared Photodetectors for MWIR & LWIR

Trilok Kumar Parashar
University Polytechnic, Birla Institute of Technology, MESRA, Ranchi

Abstract:
A theoretical model has been developed to compute some basic parameters of HgCdTe material. Also the effect mole fraction (x) on carrier concentration of HgCdTe material has been investigated.Since higher cutoff wavelength ($^{a}_{c}$ = 1.24/Eg) is inversely proportional to bandgap energy E_g, variable bandgap of HgCdTe varies cutoff wavelength (for which it can be used as detector material). Result reviles that net value of mole fraction ***(x=0.27)*** *than we found Detectivity (=4.9×108 mHz$^{1/2}$/W) and efficiency obtained on the basis of this model lies in wavelength range 7 µm - 9µm wavelength (MWLIR) and mole fraction* ***(x=0.19)*** *than we found the detectivity, D = 10.5×108 mHz$^{1/2}$/W. Therefore this Photodetector performs (LWIR) best in the wavelength range 16 µm to 18 µm.This reveals that $Hg_{1-x}Cd_xTe$ material is best suited material of Photodetector for toxic gas monitoring lies in MIIR &LWIR detection.*

I - INTRODUCTION

In this work, the choice of photosensitive materials for a Photodetector depends on the desired wavelength region of operation has been discusses. The wavelength range in which a Photodetector can perform well is basically decided by the bandgap of the material used to fabricate the Photodetector. The theoretical value of the long wavelength cutoff cannot be selected randomly for the fabrication of photodetector. It obeys certain rules/formulae. Important parameter for it is absorption coefficient (α). This material can be use in a particular wavelength range as shown in equation

$$P = P_0 \exp(-\alpha t) \qquad [1]$$

Where P_o - Incident optical power level

P –Final optical power level

α – Absorption coefficient

Optical absorption coefficient of the material is a function of wavelength. So, all material has a higher cutoff wavelength. The detection wavelength can be calculated by using the band gap energy E_G in the following equation [16].

` $$^{a}(\text{«}m) = \frac{1.24}{E_G(eV)} \qquad [2]$$

Where λ – Detection wavelength

E_G – Band gap energy

In the wavelength regions of interest such as SWIR, MWIR, and LWIR, different ternary and quaternary alloys of III-V and II-VI materials are most widely used. Differences in materials and their compositions have profound effect on behavior of material as an IR detector. IR detectors are static sensitive, fragile and environmental sensitive. Hence they should be handled with caution. Various materials are used for detection. Silicon, gallium arsenide, MCT (HgCdTe ternary alloy) and lead salts are amongst most commonly used Material [11].

Suitable materials for IR

a) III-V materials (e. g. GaAs, InAs, InSb, InP, InAsSb, AlGaAs, InGaAs)

b) II-VI Materials (e.g. HgCdTe, HgZnTe, HgMnTe)

International Journal of Engineering Technology Science and Research
IJETSR
www.ijetsr.com
ISSN 2394 – 3386
Volume 4, Issue 11
November 2017

c) IV-VI materials (e. g. PbSe, PbS, PbSnTe, PbSnSe)

The ternary alloy $InAs_{1-x}Sb_x$ is better composition for photodiodes (mostly for the 3 μm –5 μm regions) have been fabricated on InAs, InSb and GaSb substrates **.** Furthermore, the reported electron mobility for the undoped InAsSb materials is much higher compared with GaAs **[9].** As InAsSb is the most promising material for fabrication of detector for application in SWIR (1-3 µm) and MWIR (3-8 µm) application, HgCdTe has proved best material in MWIR, LWIR and VLWIR applications.MCT detectors have been the most important semiconductor for mid and long-wavelength (3 µm - 30 µm) infrared photodetectors[10]-[14].

Medium Wavelength Infrared (MWIR) or Mid-Infrared Region (MIR): Slightly longer in wavelength and covering from 3 to 8 µm. Space systems use this band to detect and track objects through booster burn out against an Earth back ground.

Long Wavelength Infrared (LWIR) or Far Infrared Region (FIR): LWIR covers spectral range from 8 to 17 µm. The long wave length band is used by space sensors to see objects above the horizon against a cold space background and beyond 17 µm and typically ends around 30 mm band cover Very Long Wavelength Infrared Region (VLWIR)

Need of Toxic gas detection:

The potential of toxic releases and adverse consequences on the environment due to a chemical accident needs for further improvement of safety measure in all processes /procedures and adoption of appropriate methods for handling hazardous chemicals. Large quantities of chemicals are also stored/ possessed in industries that are located in densely populated areas- inappropriate and haphazard construction and lack of awareness and preparedness on the part of the community further enhance their vulnerability of chemical disaster. The Bhopal Gas tragedy of 1984, the worst chemical disaster in history, where over 20,000 people died due to accidental release of toxic gas Methyl Isocyanides, is still fresh in our memories. Such accidents are significant in terms of injuries, pain, and suffering, loss of lives and damage of property environment. A small accident occurring at the local level may be a prior warning signal for impending and disaster.

Major accident can be caused by flammable and toxic substances, if the storage and handling is not proper. Accidents due to toxic release are more common in chemical industries than fire and explosion by flammable substances. Thus, monitoring of toxic gas is essential to avoid the damage and hassle. The safety arrangements can be developed by suitable sensors with IR photodetectors. The present investigation provides a theoretical approach for such type of gas detectors. The toxic gas cloud composed mainly of gases denser than the surrounding air, stayed close to the ground and spread outwards through the surrounding community. There are different kinds of toxic gases which need to be detected at different situations for different needs; Toxic gas is a gas that can damage a living and non-living organisms [6]-[7] & [15].Some toxic gases and its detection wavelength are listed in Table 1.

Table 1. Toxic gases and its detection wavelength

Gas	Absorption wavelength($\lambda\mu$m)	Gas	Absorption wavelength λ (μm)
CO_2	4.2μm	CO	4.6 µm
O_3	9.5μm	NH_3	2.3 µm
CH_4	3.3 µm	H_2S	2.7 µm
N_2O	17.0μm	HF	1.3 µm
NO_2	7.8 µm	HCl	3.6 µm

International Journal of Engineering Technology Science and Research
IJETSR
www.ijetsr.com
ISSN 2394 – 3386
Volume 4, Issue 11
November 2017

Adverse effects of toxic gases:

i. The initial effects of toxic gases are coughing, vomiting, severe eye irritation and a feeling of suffocation. Reported and studied symptoms are eye problems, respiratory difficulties, immune and neurological disorders, cardiac failure secondary to lung injury, female reproductive difficulties and birth defects.

ii. People cannot tolerate a high concentration of ammonia in air because it creates irritation.

iii. Short-term exposures of Sulphur dioxide can cause irritation of the nose and throat.

iv. Methane (CH_4) is harmful to human health and a contributing factor to global warming.

v. CO and CO_2, the major gases which are present in the exhaust gases from the automobiles, are the main cause of lungs infection and TB, seriously affect the growth of children.

vi. It is estimated that 20,000 have died since the accident from gas-related diseases. Another 100,000 to 200,000 people are estimated to have permanent injuries. The quality of the epidemiological and clinical research varies.

Detection method for Toxic gases:

So for this there are certain methods for the detection of gases on the basis of their wavelengths because each gas has its certain wavelength range. For detection of toxic gases optical fiber gas sensors are the best. Optical fiber gas sensors have the advantages of high sensitivity, fast response, freedom from electromagnetic influence and immunity to combustion and explosion [6]-[8] & [15]**.**

. II - ANALYTICAL MODELING

Numerical computations have been carried out on p^+-$Hg_{0.73}Cd_{0.27}Te$/ n- $Hg_{0.73}Cd_{0.27}Te$/ CdZnT p^+n homojunction Photodetector at 77K for operation at LWIR. The light has been assumed to be incident on the top p^+- $Hg_{0.73}Cd_{0.27}Te$ side of the Photodetector. The photons with energy higher than the energy gap create electron-hole pairs in p and n region. The band gap of $Hg_{1-x}Cd_xTe$ as a function of temperature T and alloy composition x is included in the simulation model using the empirical formula [1-2].

Quantum Efficiency

The quantum efficiency (η) of a p-n junction Photodetector has generally three major components. These components arise from the contribution of the three regions e.g., neutral n-region (η_n), neutral the optical generation p-region (η_p) and the depletion region (η_{dep}) rate of electron-hole pairs, as a function of distance x from the surface can be written as [1]

$$\eta = \eta_n + \eta_p + \eta_{dep} \qquad [3]$$

Specific Detectivity

The most important figure of merit of the Photodetector for use toxic gas monitoring is the specific detectivity D^*[1], which depends on the wavelength of incident light λ, the quantum efficiency η and zero bias resistance area products (R_0A).

$$D^* = \frac{q\eta a}{hc}\sqrt{\frac{R_0 A_{net}}{4kT}} \qquad [4]$$

International Journal of Engineering Technology Science and Research
IJETSR
www.ijetsr.com
ISSN 2394 – 3386
Volume 4, Issue 11
November 2017

Responsivity

The responsivity ($\Re$) of the Photodetector depends on the wavelength of incident light λ, the quantum efficiency η [1]. The equation to obtain responsivity is given as

$$\Re = \frac{\eta q a}{hc} \qquad [5]$$

III - RESULTS AND DISCUSSIONS

Numerical computations have been carried out on p^{+-} $Hg_{0.73}Cd_{0.27}Te$/ n^{-} $Hg_{0.73}Cd_{0.27}Te$/ CdZnT $p^{+}n$ homojunction photodetector at 77K for operation at LWIR. The light has been assumed to be incident on the top p+- $Hg_{0.73}Cd_{0.27}Te$ side of the photodetector. The photons with energy higher than the energy gap create electron-hole pairs in p and n region. The band gap of $Hg_{1-x}Cd_xTe$ as a function of temperature, T and alloy composition, x is included in the simulation model using the empirical formula. The intrinsic carrier concentration formula has taken as In present the gas detectors such as Detectivity and quantum efficiency on the applied wavelength has been estimated quantitatively. The quantum efficiency and specific Detectivity are the two main device parameter in terms of which the performance of the detector is described [1]-[2].

Numerical computations have been carried out on $p^{+-}Hg_{0.81}Cd_{0.19}Te$ / $n^{-}Hg_{0.81}Cd_{0.19}Te$/ CdZnT $p^{+}n$ homojunction photodetector at 77K for operation at LWIR. Absorption coefficient can be written as [12]-[13].

$$\sim = \sim_0 \exp[\frac{\pm (E - E_0)}{T + T_0}] \qquad \pm = 3.267 \times 10^4 (1 + x) \qquad [6]$$

Where $\alpha_0 = \exp(53.61x - 18.88)$, $E_0 = -0.3424 + 1.838x + 0.148x^2$ (eV), $T_0 = 81.9$ (K), are fitting parameters which vary smoothly with composition. Fig.2, shows the variation of the absorption coefficient of HgCdTe versus the operating wavelength. The material exhibits an absorption coefficient up to 25 μm. The absorption coefficient decreases sharply near the long wavelength cut-off.

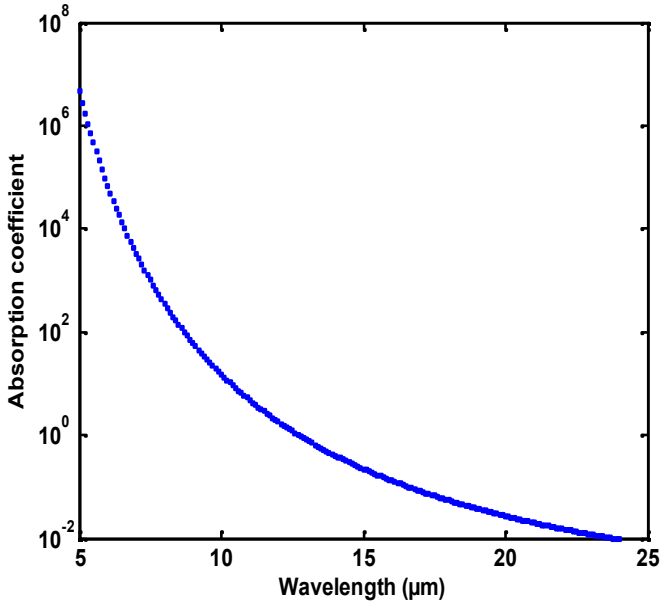

Fig.2. absorption coefficient with respect to wavelength

International Journal of Engineering Technology Science and Research
IJETSR
www.ijetsr.com
ISSN 2394 – 3386
Volume 4, Issue 11
November 2017

A - Modelling of Detector (Mole fraction,x=0.27)

Structure consists of highly doped p+-$Hg_{0.73}Cd_{0.27}Te$ (Mole over lightly doped n-$Hg_{0.73}Cd_{0.27}Te$ shown in Fig.1. which is virtually grown on a suitable substrate such as CdZnTe. The light has been assumed to be incident on the top p+- $Hg_{0.73}Cd_{0.27}Te$ side of the photodetector to collect large quantity of illumination.

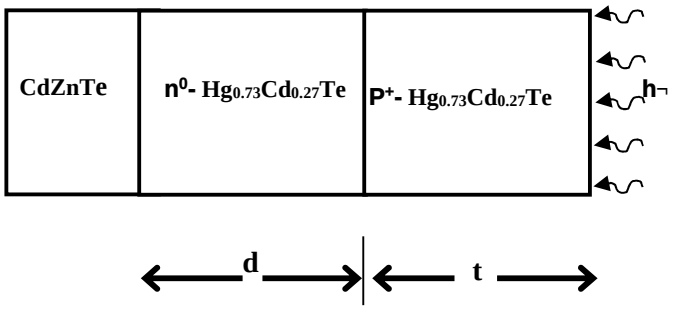

Fig.1. Structure of the photodetector and different dark current components

. In present work the variation of the major parameters of the gas detectors such as quantum efficiency, responsivity and detectivity with the applied wavelength has been estimated quantitatively.

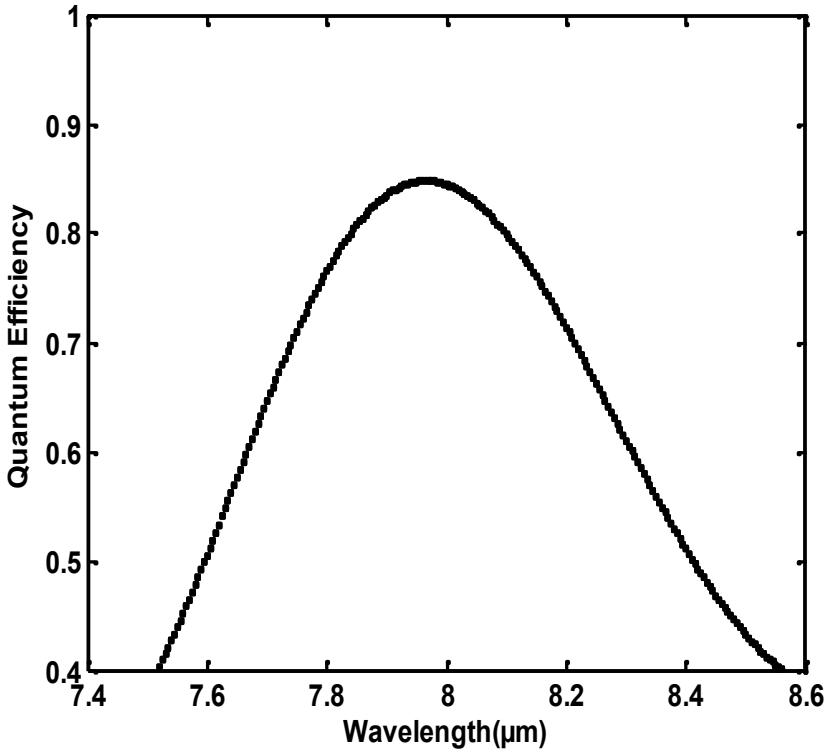

Fig. 3. Quantum Efficiency with respect to operating wavelength

.

International Journal of Engineering Technology Science and Research
IJETSR
www.ijetsr.com
ISSN 2394 – 3386
Volume 4, Issue 11
November 2017

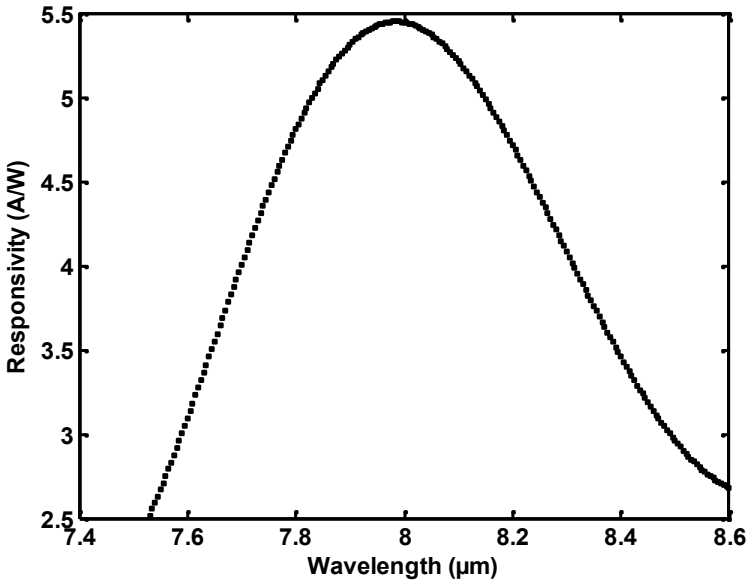

Fig. 4. Responsivity with respect to operating wavelength

Fig. 3, variation of the efficiency of the detector with respect to operating wavelength has been presented. In present case, the efficiency of the detector achieves its maximum value ~ 0.80 at ranges 7 µm to 9 µm and it decreases sharply on the both side. One can see that the efficiency wavelength ranges 7 µm to 9 µm which may be consider the range over which the device can be utilise as detector.

In Fig.4, variation of the responsivity of the detector with respect to operating wavelength has been presented. Here also the peak responsivity ≈5.5 A/W is obtained at ranges 7 µm to 9 µm.

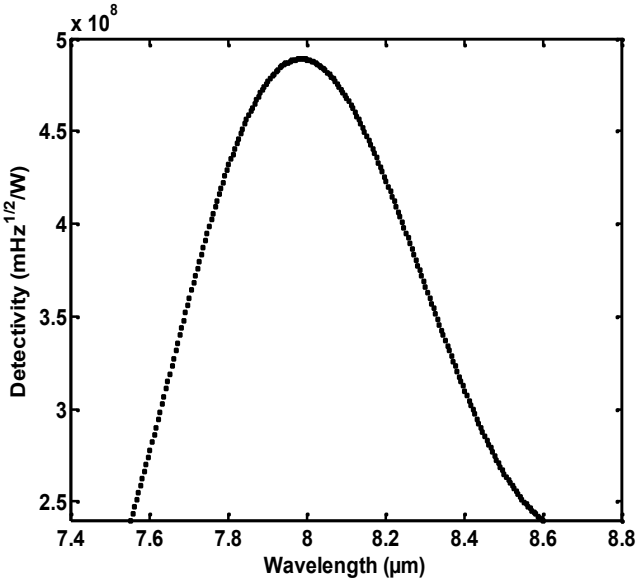

Fig. 5. Detectivity with respect to operating wavelength

The variation of detectivity of a detector with respect to operating wavelength shown in figure 5, the peak detectivity (~4.9×10^8 $mHz^{1/2}/W$) is obtained at ranges 7 µm to 9 µm. For non telecommunication

International Journal of Engineering Technology Science and Research
IJETSR
www.ijetsr.com
ISSN 2394 – 3386
Volume 4, Issue 11
November 2017

applications such as gas sensor device can be utilised as detector for gas whose characteristic wavelength is ranges 7 µm to 9 µm like nitrous oxide (NO_2) whose characteristic wavelength is 7.8 µm.

B - Modelling of Detector (Mole fraction,x=0.19)

We found that $Hg_{1-x}CdxTe$ and $p^{+-}Hg_{0.81}Cd_{0.19}Te$ layer the performance of the device has been examined by self generated MATLAB.

In Figure 6, variation of the efficiency of the detector with respect to operating wavelength has been presented. In present case, the efficiency of the detector achieves its maximum value ~ 0.90 at the wavelength ranges 16 µm to 18 µm. It decreases sharply on the both side. One can see that the efficiency is more than 0.85 between the wavelength ranges 16 µm to 18 µm.

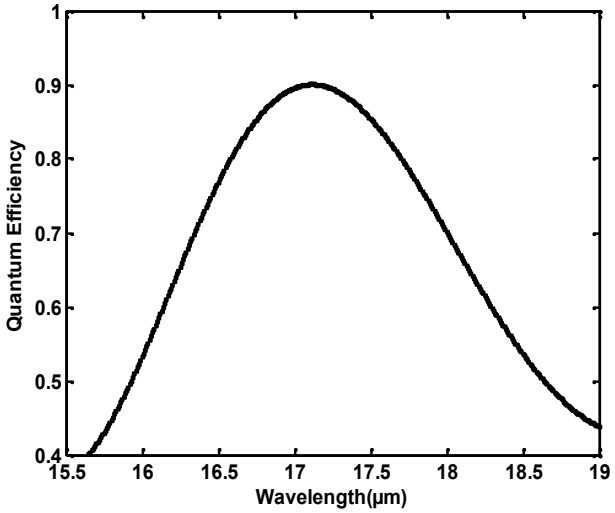

Fig.6, Efficiency with respect to operating wavelength

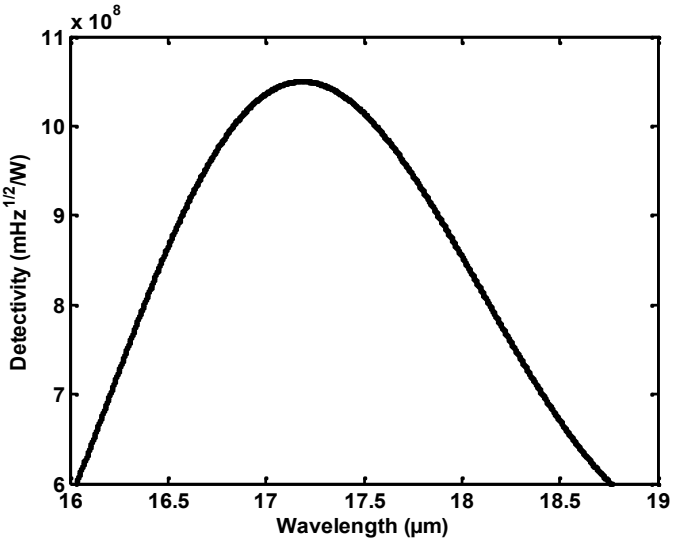

Fig. 7, Detectivity with respect to operating wavelength

The variation of detectivity of detector with respect to operating wavelength shown in Fig.7; here the peak detectivity (~10.5×10^8 $mHz^{1/2}/W$) is obtained at wavelength ranges 16 µm to 18 µm and its emissions are mainly determined by food supply, because these emissions largely stem from soil processes induced by

International Journal of Engineering Technology Science and Research
IJETSR
www.ijetsr.com
ISSN 2394 – 3386
Volume 4, Issue 11
November 2017

agriculture. Like CH_4, N_2O emissions are generally highest in the regional wealth scenario. N_2O emissions are generally affected by large uncertainties, because these are mainly caused by bacterial soil processes and are therefore difficult to measure. Extensive research into N_2O detectors are still a major required. The present work is a small contribution in this direction. On the basis of the result obtained from the present work we can say that this detector is best suited for detection wavelength ranges 16 µm to 18 µm. For non telecommunication applications such as gas sensor device can be utilised as detector for whose characteristic wavelength ranges is 16 µm to 18 µm 17µm such as Signature wavelength of the nitrous oxide gas, N_2O is 17 µm.

CONCLUSION

An analytical modeling of first Structure p+-$Hg_{0.73}Cd_{0.27}Te$/n0-$Hg_{0.73}Cd_{0.27}Te$/CdZnTe, homojunction photodetector for long wavelength free space optical communication has been reported.. Results of our study reveal that suitable biasing conditions the photodetector exhibits the high detectivity (=4.9×10^8 $mHz^{1/2}/W$) and efficiency obtained on the basis of this model lies in wavelength range 7 µm - 9µm wavelength, when mole fraction is **(x=0.27),** which reveals that this detector is best suited for MWIR detection of gases such as NO_2 (7.8 µm), H_2O (7.7 µm), C_2H_2 (7.6 µm).

And modeling of Second Structure **$Hg_{0.81}Cd_{0.19}Te$,** We found that when mole fraction is **(x=0.19)** We got high efficiency maximum value ~ 0.85 and high detectivity, D = 10.5×10^8 $mHz^{1/2}/W$ at the wavelength range 16 µm to 18 µm. Therefore this photodetector best performs in LWIR gas detection; like N_2O gas (Characteristic wavelength N_2O is 17µm). The band gap tunability with mole fraction(x), $Hg_{1-x}Cd_xTe$ has evolved to become the most important/versatile material for detector applications over the entire IR range. Thus HgCdTe material is best matetial for non telecommunication applications such as gas sensor device can be utilized as detector for MWIR and LWIR with changing the mole fraction x.

REFERENCES

[1]. T.K.Parashar and R.K.Lal, "Modeling and Simulation of HgCdTe based Photodetector for N_2O gas detection", Journal of Electron Devices, Vol. 11, pp. 527-537, (2011).

[2] T.K.Parashar and R.K.Lal "Theoretical modelling of InP based photo detector for hydrogen fluoride gas detection in short wavelength region", OPTOELECTRONICS AND ADVANCED MATERIALS – RAPID COMMUNICATIONS Vol. 5, No. 7, pp. 732 – 737, July 2011.

[3] A Rogalski, J Antoszewski and L Faraone, "Third-generation infrared photodetector arrays," J. Appl. Phys. 105, 09110 (2009).

[4]. Chang Y, Grein C H, Zhao J, Becker C R, Flatte M E, Liao P K, Aqariden F and Sivananthan S. "Carrier recombination lifetime characterization of molecular beam epitaxially grown HgCdTe," Appl. Phys. Lett. **93**, 192111 (2008).

[5]. A Zemel, I Lukomsky and J. E Weiss. "Mechanism of carrier transport across the junction of narrow band-gap planar n+p HgCdTe photodiodes grown by liquid-phase epitaxy," J Appl.Phys, **98**, 054504 (2005).

[6] . Mello, M., Poti1, B, Risi,,A de Passaseo, A, Lomascolo M. and Vittorio, M. De, "GaN optical system for CO and NO gas detection in the exhaust manifold of combustion engines," J. Opt. A: Pure Appl. Opt. **8**, S545–S549 (2006).

[7] M Mello, B Poti1, A Risi, A de Passaseo, M Lomascolo and M. De Vittorio, "GaN optical system for CO and NO gas detection in the exhaust manifold of combustion engines," J. Opt. A: Pure Appl. Opt. **8**, S545–S549 (2006).

[8] Le Perchec J, Y Desieres and Espiau de R Lamaestre,"Plasmon-based photosensors comprising a very thin semiconducting region," J. Appl. Phys. Lett, 94, 181104 (2009).

[9] Xiaoming Liu, Hongtao Li, Fengyun Guo, Meicheng Li, Liancheng Zhao,. Effect of annealing on electrical properties of InAsSb films grown on GaAs substrates by molecular beam epitaxy. Physica E 41, pp. 1635–1639 (2009).

[10] M.H. Weiler, "Magnetooptical properties of Hg1-xCdxTe Alloyed," in Semiconductors and Semimetals, edited by R.K. Willordson And A.C. Beer, Academic Press, New York **16**, 119 (1981).

[11] Rogalski, A., New material systems for third generation infrared detectors. Opto-Electronics Review, 16 (4), 458–482(2008).

[12] Chu, J. Li., S.S. & Singh A., Investigation of Broadband Quantum Well Infrared Photodetector for 8-14 µm Detection. IEEE J. of Quantum Electronics, 35, 5, 312-319. (1999).

[13] J. P Rosbeck,., R. E., Star, , S. L Price., and , K J Riley.,. Background and temperature dependent current–voltage characteristics of Hg1−xCdxTe photodiodes. J. Appl. Phys. 53 6430–40. (1982).

[14] M A Kinch Fundamental physics of infrared detector materials J. Electron. Mater. **29**, 809 (2000).

[15] Uehara, K., and Tai, H., Remote detection of methane using a 1.66 µm, diode laser. Appl.Opt. 31, 809-814.(1992).

[16] S.O Kasap, “Optoelectronics and Photonics, Principles and Practices”; Prentice Hall, p. 221 (2001).